

Structural analysis of mono- and bis-sulfated glycosphingolipids by negative liquid secondary ion mass spectrometry with high- and low-energy collision-induced dissociation [☆]

Keiko Tadano-Aritomi ^{a,*}, Harumi Kubo ^b, Philip Ireland ^c, Masaru Okuda ^a, Takeshi Kasama ^d, Shizuo Handa ^e, Ineo Ishizuka ^a

^a *Department of Biochemistry, Teikyo University School of Medicine, Kaga 2-11-1, Itabashi-ku, Tokyo 173, Japan*

^b *Shimadzu Corporation, Nakagyo-ku, Kyoto 604, Japan*

^c *Kratos Analytical, Urmston, Manchester M31 2LD, UK*

^d *Laboratory for Biomedical Analysis, Faculty of Medicine, Tokyo Medical and Dental University, Bunkyo-ku, Tokyo 113, Japan*

^e *Department of Biochemistry, Faculty of Medicine, Tokyo Medical and Dental University, Bunkyo-ku, Tokyo 113, Japan*

Received 11 November 1994; accepted 22 February 1995

Abstract

Several underivatized mono- and bis-sulfated glycosphingolipids having ganglioside or gangliotetraose core structure were analyzed by negative liquid secondary ion mass spectrometry (LSIMS) with high- and low-energy collision-induced dissociation (CID). In the normal negative LSIMS spectra, each mono-sulfated glycolipid gave abundant $[M - H]^-$ ions and each bis-sulfated glycolipid gave abundant $[M + Na - 2H]^-$ ions as well as the hydrogen sulfate anion $[OSO_3H]^-$. In high-energy CID spectra of the deprotonated molecule, only ions containing a sulfate ester were clearly observed. When a sulfate was present on the non-reducing terminal saccharide residue, a series of ions corresponding to sulfated mono- to tetra-saccharides, resulting from sequential cleavage of glycosidic bonds, were observed. If the sulfate was attached to an internal hexose of the sugar chain, the product ions corresponding to the non-sulfated, non-reducing terminal residue were absent. In contrast, the low-energy CID resulted in extremely simple spectra that contained

[☆] Part of this study was presented at the VII European Carbohydrate Symposium, August 1993, in Cracow, Poland.

* Corresponding author.

only one or two major product ions characteristic of each sulfated glycolipid. These results provided clear information on the overall sugar and ceramide compositions, and allowed saccharide structures differing in location and number of sulfate esters to be distinguished.

Keywords: Sulfolipids; Glycosphingolipids; Mass spectrometry; Liquid SIMS; Collision-induced dissociation (CID)

1. Introduction

Sulfated glycolipids are a class of acidic glycolipids containing one or two sulfate esters on their oligosaccharide chains [2]. Next to nervous tissue, the highest concentrations of sulfated glycolipids occur in kidney, suggesting a role of these sulfated glycolipids in adaptation to the environmental osmolarity [3–5]. To clarify the association of sulfated glycolipids with renal functions, characterization of the chemical structure of the glycolipids is a fundamental requirement. The kidney of rat contains a large variety of sulfated glycosphingolipids in addition to the two well-known sulfated glycolipids, galactosylceramide sulfate (SM4s¹) [6] and lactosylceramide sulfate (SM3) [7]. Since 1982, we have isolated seven novel sulfated glycosphingolipids belonging to the ganglio-series [8–12] and isoglobo-series core structures [13,14]. All have one or two sulfate esters at C-3 of galactose or *N*-acetylgalactosamine (Table 1). In most cases, the content of the glycolipid is low, and purification and complete characterization are cumbersome and time-consuming.

The continuous development of instrumentation in mass spectrometry, as well as the availability of soft ionization methods like fast atom bombardment (FAB) and liquid secondary ion mass spectrometry (LSIMS), have made it possible to analyze glycoconjugate structures [15–21] without the derivatization required for electron [22] and chemical ionization. We have explored the use of LSIMS in the negative ion mode for the analysis of underivatized sulfated glycosphingolipids [13,14]. In the present study we report that several homologous sulfated glycolipids, when analyzed by collision-induced dissociation (CID), form product ions which reflect structural differences in the position and number of sulfate esters, as well as the carbohydrate sequence.

2. Experimental

SM2a [8], SM2b [12], SB2 [9] and SB1a [10] were purified from rat kidney and SM1a was prepared by solvolysis of SB1a [10]. SM1b was isolated from mouse small intestine [23].

¹ Abbreviations for sulfated glycolipids follow the modifications of the nomenclature system of Svennerholm for gangliosides [1]: SM4s, galactosylceramide sulfate, GalCer I³-sulfate; SM3, lactosylceramide sulfate, LacCer II³-sulfate; SM2a, Gg3Cer II³-sulfate; SM2b, Gg₃Cer III³-sulfate; SB2, Gg₃Cer II³,III³-bis-sulfate; SM1a, Gg₄Cer II³-sulfate; SM1b, Gg₄Cer IV³-sulfate; SB1a, Gg₄Cer II³,IV³-bis-sulfate; GM1a, II³NeuAc-Gg₄ Cer; Cer, ceramide; HFA, 2-hydroxylated fatty acid; LSIMS, liquid secondary ion mass spectrometry; CID, collision-induced dissociation; CRF, charge-remote fragmentation; MS/MS, tandem mass spectrometry.

LSIMS was carried out on a CONCEPT IH forward-geometry mass spectrometer (Shimadzu/Kratos, Kyoto) in the negative ion mode [13,14,24]. The acceleration voltage was maintained at 8 kV during all experiments and the primary ion beam was cesium (14 keV). The matrices used were triethanolamine for mono-sulfated glycolipids and 3-nitrobenzyl alcohol for bis-sulfated glycolipids. The mass range and resolution for normal LSIMS were m/z 50–1600 and 1000, respectively. Linked scan spectra were obtained at constant B/E ratio after CID with air introduced into a collision cell in the first field-free region between the ion source and the electrostatic sector [14,24]. The pressure in the collision cell was not known, but the admission of collision gas reduced the precursor ion intensity by a factor of 10. About 500 pmol of underivatized sulfated glycolipid in MeOH was applied onto the target together with $\sim 1 \mu\text{L}$ of matrix. The scan speed for both normal and linked scan was 5 s/decade.

The negative LSIMS spectra were also run on a TSQ 70 triple-stage quadrupole mass spectrometer (Finnigan MAT Inc., San Jose, CA) equipped with a cesium gun [13]. The kinetic energy of the primary ion beam was 20 keV. The detection of the secondary ions was performed by a 20-keV ion conversion dynode and electron multiplier. About 1 nmol of each compound dissolved in CHCl_3 –MeOH (1:2, v/v) was mixed on the target with 0.5 μL triethanolamine as the matrix. Low-energy CID MS/MS studies were performed with a 10-eV collision energy and 1.5×10^{-3} torr of argon as the collision gas [25]. The spectra were recorded in the m/z 50–1600 Da region at the scan rate of 250 Da/s.

3. Results and discussion

Negative LSIMS.—Table 1 shows the structures of the mono- and bis-sulfated glycosphingolipids used in this study. They are homologous sulfated glycosphingolipids based on gangliotriaose and gangliotetraose core with a 3-*O*-sulfated galactose and/or 3-*O*-sulfated *N*-acetylgalactosamine in their oligosaccharide chains. The ceramide of these sulfated glycolipids consists mainly of 4-hydroxysphinganine (t18:0) and non-hydroxylated fatty acids [8–10,12], except for SM1b which has 2-hydroxylated fatty acids [23].

Fig. 1 shows the LSIMS spectra of mono-sulfated glycolipid, SM2b, and bis-sulfated glycolipid, SB2. The ion at m/z 97, corresponding to the hydrogen sulfate anion (HSO_4^-), was one of the abundant fragment ions [13,14,23,26–28]. In the high mass region, SM2b gave abundant $[\text{M} - \text{H}]^-$ ions corresponding to the molecular weight of mono-sulfated gangliotriaosylceramide containing a ceramide with mainly trihydroxy C18 base (t18:0) and non-hydroxy C24:0 (m/z 1273), C22:0 (m/z 1245), and C20:0 (m/z 1217) fatty acids. On the other hand, the spectrum of SB2 exhibited abundant $[\text{M} + \text{Na} - 2\text{H}]^-$ ions at m/z 1319–1375 corresponding to the molecular weight of bis-sulfated gangliotetraosylceramide with t18:0 base and C20–24 fatty acids [15]. These molecule related ions, $[\text{M} - \text{H}]^-$ for mono-sulfated glycolipids and $[\text{M} + \text{Na} - 2\text{H}]^-$ for bis-sulfated glycolipids, were observed for all sulfated glycosphingolipids used in this study and made it possible to deduce the combination of fatty acids and sphingoid bases present in the various molecular species. The response of the $[\text{M} + \text{Na} - 2\text{H}]^-$ ion for

bis-sulfated glycolipids was 10 times more intense in 3-nitrobenzyl alcohol matrix than in triethanolamine (data not shown). It was reported recently that both $[M - H]^-$ and $[M + Na - 2H]^-$ ions were produced in the negative ion FAB spectrum of bis-sulfated oligosaccharides [29,30]. In the spectra reported here, however, only $[M + Na - 2H]^-$ ions can be clearly observed in the negative ion LSIMS spectra.

The magnified molecular ion region for each sulfated glycolipid can be seen in Fig. 2. As mentioned above, a series of $[M - H]^-$ ions was detected for each mono-sulfated glycolipid (SM2a and SM1a), and a series of $[M + Na - 2H]^-$ ions was observed for each bis-sulfated glycolipid (SB2 and SB1a). In the case of SB2 and SB1a, the loss of a

Table 1

Compounds studied and their major ceramide compositions

Gangliotriaose core

SM2a ^a	$\begin{array}{c} \text{HSO}_3 \\ \\ 3 \\ \text{GalNAc}\beta 1-4\text{Gal}\beta 1-4\text{Glc}\beta 1-1\text{Cer} \end{array}$ (C24:0 ^b /t18:0 ^c)
SM2b	$\begin{array}{c} \text{HSO}_3 \\ \\ 3 \\ \text{GalNAc}\beta 1-4\text{Gal}\beta 1-4\text{Glc}\beta 1-1\text{Cer} \end{array}$ (C24:0 ^b /t18:0 ^c)
SB2	$\begin{array}{cc} \text{HSO}_3 & \text{HSO}_3 \\ & \\ 3 & 3 \\ \text{GalNAc}\beta 1-4\text{Gal}\beta 1-4\text{Glc}\beta 1-1\text{Cer} \end{array}$ (C24:0 ^b /t18:0 ^c)

Gangliotetraose core

SM1a	$\begin{array}{c} \text{HSO}_3 \\ \\ 3 \\ \text{Gal}\beta 1-3\text{GalNAc}\beta 1-4\text{Gal}\beta 1-4\text{Glc}\beta 1-1\text{Cer} \end{array}$ (C24:0 ^b /t18:0 ^c)
SM1b	$\begin{array}{c} \text{HSO}_3 \\ \\ 3 \\ \text{Gal}\beta 1-3\text{GalNAc}\beta 1-4\text{Gal}\beta 1-4\text{Glc}\beta 1-1\text{Cer} \end{array}$ (C24h:0 ^d /t18:0 ^c)
SB1a	$\begin{array}{cc} \text{HSO}_3 & \text{HSO}_3 \\ & \\ 3 & 3 \\ \text{Gal}\beta 1-3\text{GalNAc}\beta 1-4\text{Gal}\beta 1-4\text{Glc}\beta 1-1\text{Cer} \end{array}$ (C24:0 ^b /t18:0 ^c)

^aSM2a, Gg₃Cer II³-sulfate; SM2b, Gg₃Cer III³-sulfate; SB2, Gg₃Cer II³,III³-bis-sulfate; SM1a, Gg₄Cer II³-sulfate; SM1b, Gg₄Cer IV³-sulfate; SB1a, Gg₄Cer II³,IV³-bis-sulfate. ^bC24 non-hydroxylated fatty acid (tetracosanoic acid). ^c4-hydroxysphinganine. ^dC24 2-hydroxylated fatty acid (2-hydroxytetracosanoic acid).

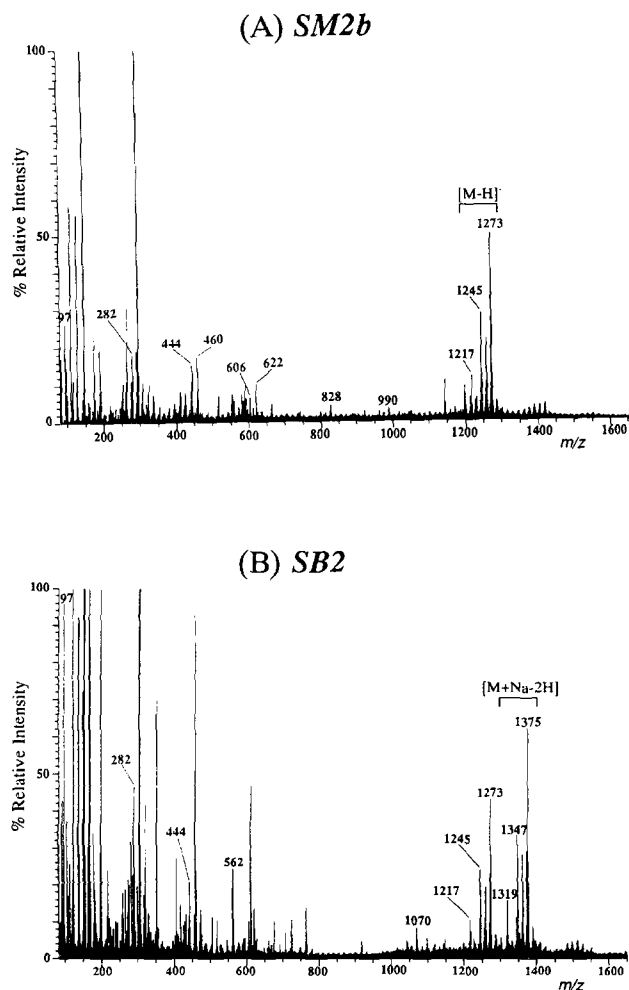


Fig. 1. Negative LSIMS spectra of mono- and bis-sulfated glycolipids with ganglioside core. (A) SM2b in triethanolamine matrix. (B) SB2 in 3-nitrobenzyl alcohol matrix.

sodium sulfate moiety (102 Da) through fragmentation yielded a series of $[M - \text{SO}_3\text{H}]^-$ ions (Fig. 2, lower two spectra), which were identical to the $[M - \text{H}]^-$ ions of the corresponding mono-sulfated glycolipids, SM2a and SM1a (Fig. 2, upper two spectra), respectively. Additional series of fragment ions corresponding to the sulfated di- and trisaccharide plus ceramide (m/z 1070 and 1273, Fig. 2) were observed for SM2a, SB2, SM1a and SB1a, which carry an internal sulfated lactose unit. These ions, although not very abundant, are key fragments since they result from the elimination of the terminal mono- or disaccharide and therefore could demonstrate the structure, HexNAc-O-Hex-O-Hex-O-Cer, with a sulfate attached to one of its hexoses. Furthermore, the presence of the above two series of fragment ions (m/z 1070 and 1273) and the

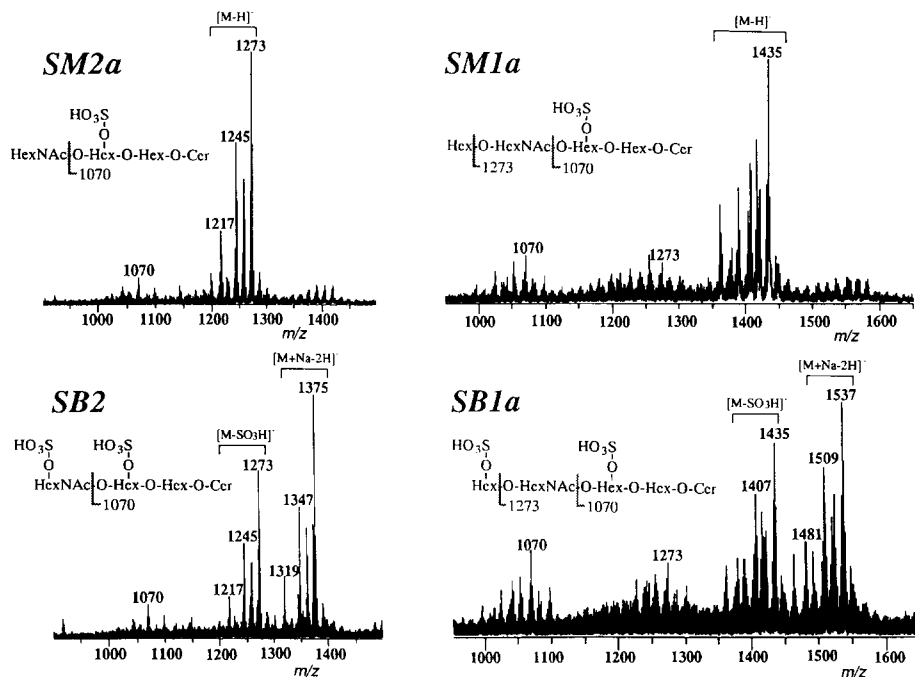


Fig. 2. Negative LSIMS molecular ion region of SM2a, SM1a, SB2, and SB1a with their respective fragmentation schemes. The matrix used for SM2a and SM1a is triethanolamine and that for SB2 and SB1a is 3-nitrobenzyl alcohol.

absence of ions corresponding to the sulfated monosaccharide plus ceramide, $\text{HSO}_3\text{-O-Hex-O-Cer}$ (m/z 908), suggest that SM2a, SB2, SM1a and SB1a have a common structure, $\text{HSO}_3\text{-O-Hex-O-Hex-O-Cer}$, rather than the alternative structures, $\text{HSO}_3\text{-O-HexNAc-O-Hex-O-Cer-O-Cer}$ or $\text{HSO}_3\text{-O-Hex-O-Cer}$.

High-energy CID.—Fig. 3 shows the negative ion LSIMS and high-energy CID spectra of SM1b. Among the sulfated glycosphingolipids used in this study, only SM1b has 2-hydroxylated fatty acids (HFA) as the major component of its ceramide [23] and one of the HFA-type molecular species, m/z 1451 (t18:0/C24h:0), was selected as the precursor ion for CID. The most intense signal at m/z 1085 was due to the loss of the fatty acid moiety from the molecular ion to yield the corresponding *N*-deacylated lyso-form of SM1b [26]. According to a recent report on FAB-MS of sulfatide (GalCer I³-sulfate) [28], the fragment ion with the lyso-form structure is derived from the HFA-type sulfatide only, at least for negative ion FAB and low-energy CID. Also, in the present case, the intense lyso-form ion was found in the high energy CID spectrum of HFA-type SM1b only and not in that of other sulfated glycolipids containing non-hydroxylated fatty acids. This ion at m/z 1085 was also observed, although at greatly reduced intensity, in the negative ion LSIMS (Fig. 3, lower spectrum) and low-energy CID (Fig. 6B) of SM1b. The spectrum also exhibited a series of ions which were consistent with sulfated mono- to tetra-saccharides, such as m/z 257, 460, 622, and 784, resulting from the sequential cleavage of the glycosidic bonds [17,18,31]. The

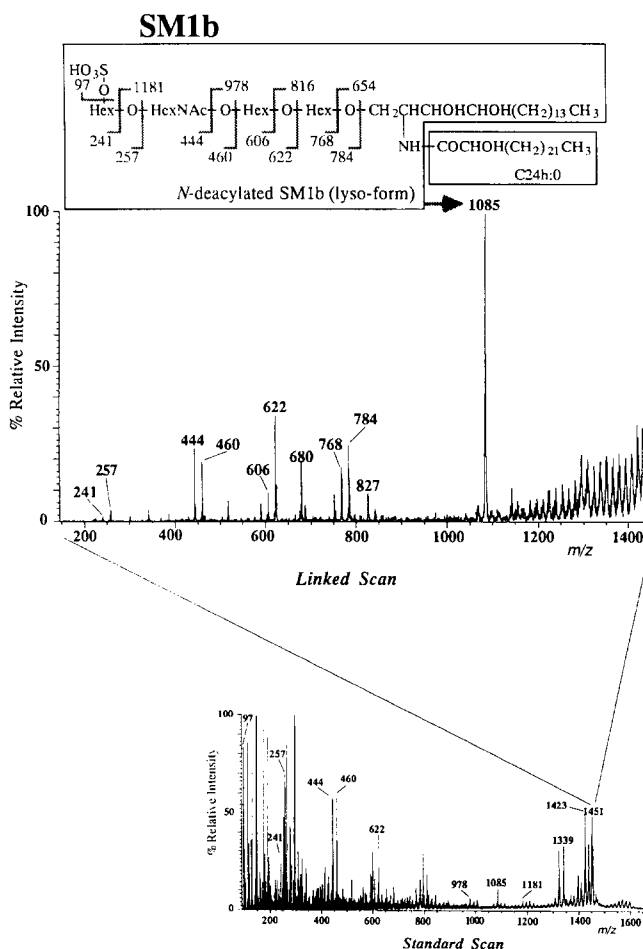


Fig. 3. Negative LSIMS (*Standard Scan*) and high-energy CID (*Linked Scan*) spectra of SM1b with its respective fragmentation scheme. The deprotonated molecule $[M-H]^-$ formed by LSIMS ionization, m/z 1451, was selected as the precursor ion.

differences between these fragments of 257, 203, 162 and 162 Da indicated the sequence: sulfated hexose, *N*-acetylhexosamine, hexose, hexose. The last ion of this series, m/z 784, represents the complete sulfated sugar moiety. The same sets of product ions were also observed for SM2b, SB2, SB1a, all of which have a sulfate on the non-reducing terminal saccharide residue. These sets of product ions demonstrated the presence of the linear sugar sequence and gave positive evidence for the presence of a ganglioseries core in these compounds.

Fig. 4 shows the negative LSIMS and high-energy CID spectra of SM1a, which has a sulfate ester on an internal hexose. One of the $[M-H]^-$ ions, m/z 1435 (t18:0/C24:0), was selected as the precursor ion for CID. In contrast to the spectrum of SM1b (Fig. 3), neither the fragments corresponding to the lyso-form nor the terminal mono- or disaccharide fragments were observed, indicating the absence of both 2-hydroxylated

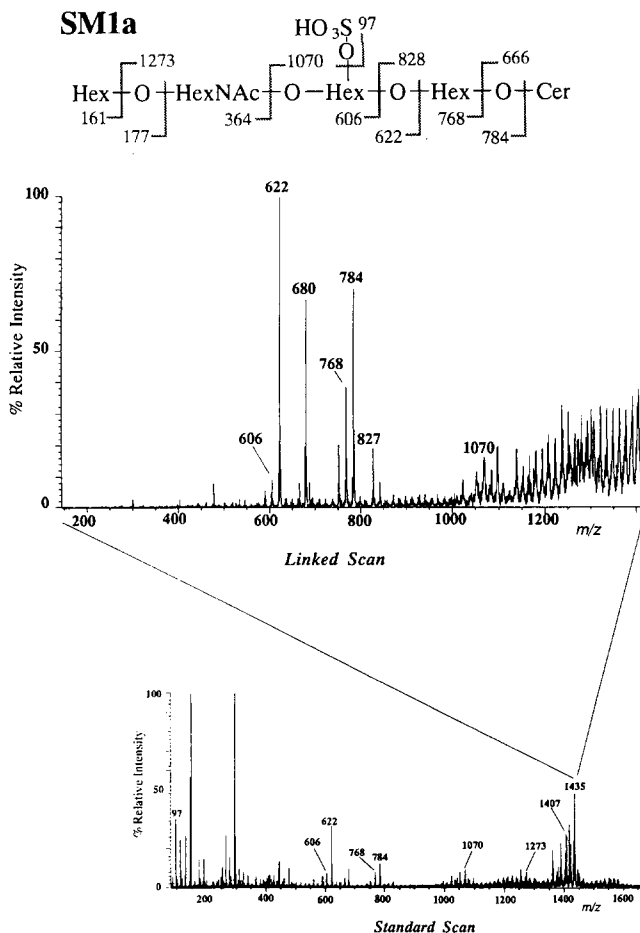


Fig. 4. Negative LSIMS (*Standard Scan*) and high-energy CID (*Linked Scan*) spectra of SM1a with its respective fragmentation scheme. The deprotonated molecule $[M-H]^-$ formed by LSIMS ionization, m/z 1435, was selected as the precursor ion.

fatty acids and a sulfate ester attached at the non-reducing terminus. Instead, there were the intense ions originating from the sulfated tri- (m/z 622) and tetra-saccharides (m/z 784).

The region of CID spectra containing the sugar product ions for three sulfated glycolipids with gangliotetraose core are compared in Fig. 5. Intense product ions derived from sulfated tri- and tetra-saccharides were observed for all of the three compounds: mono-sulfated ions at m/z 784, etc. for SM1a and SM1b (Figs 5A and 5B), and bis-sulfated ions at m/z 724, 886, etc. for SB1a (Fig. 5C). The product ions, at m/z 680 (SM1a and SM1b) and at m/z 782 (SB1a), could originate from the cleavage of the glucose ring linked to the ceramide (Fig. 5, diagram in figure legend) [31]. Other signals, m/z 827 (SM1a and SM1b) and m/z 929 (SB1a), probably originated from the sulfated oligosaccharide plus a part of ceramide, $R-O-CH=CHNH_2$

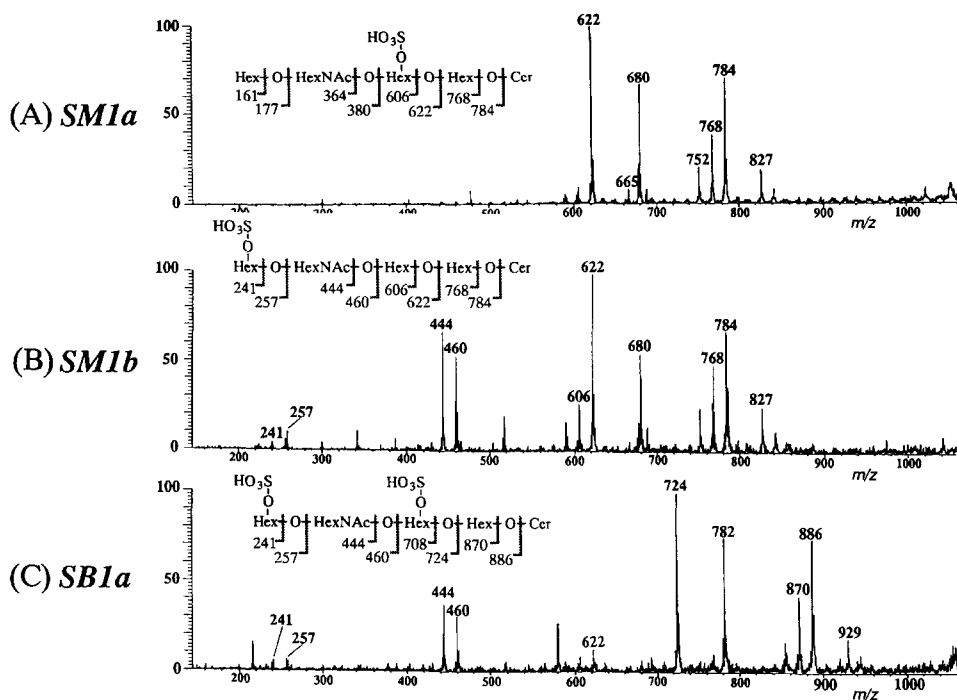
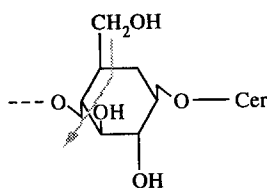


Fig. 5. The region of high-energy CID spectra containing the saccharide product ions for three sulfated glycolipids of gangliotetraose core with their respective CID schemes. The deprotonated molecules formed by LSIMS ionization, $[\text{M} - \text{H}]^-$ 1435 for SM1a (A), $[\text{M} - \text{H}]^-$ 1451 for SM1b (B) and $[\text{M} + \text{Na} - 2\text{H}]^-$ 1537 for SB1a (C), were selected as the precursor ions. The product ions at m/z 680 (A and B) and 782 (C) were produced by the cleavage of the glucose ring linked to the ceramide [31]:



(Fig. 5) [28]. The difference in spectra between these three compounds was attributed to the intensity of the mono- or di-saccharide product ions arising from the non-reducing end. Ions at m/z 241, 257, 444 and 460 were observed for SM1b (Fig. 5B) but not for its isomer SM1a (Fig. 5A). The corresponding ions for SB1a (Fig. 5C) can be observed, but at slightly reduced intensity compared to SM1b. These ions in the spectrum of SM1b, representing the presence of the structure $\text{HSO}_3\text{-O-Hex-O-HexNAC-O-}$ at the non-reducing end, exclude the possibility of the alternative structure, possessing a sulfate ester attached to an internal hexose. Similar high-energy CID spectra were obtained from another three homologous sulfated glycolipids, SM2a, SM2b and SB2, with the gangliotriaose core (data not shown).

A common characteristic of these sulfated glycolipids is that the negative charge is rigidly located in sulfate with little possibility of charge migration into the fragmenting portion of the ion. Therefore, as a result of the stable site of negative charge, structurally diagnostic cleavages of the glycosidic bonds in these sulfated glycolipids would be a result of collision-induced charge-remote fragmentations (CRF) rather than charge-mediated fragmentations [32]. Also, by CRF, the bonds distant from the charge-site were cleaved to give a pattern of peaks at high mass region, that were evenly spaced by 14 amu (Figs 3 and 4), corresponding to sequential carbon-carbon bond cleavages in the ceramide moiety [28,32].

To confirm the difference in the location of the sulfate ester between two isomeric glycolipids, SM1a and SM1b, the ion corresponding to the whole sugar region without ceramide, m/z 784, was selected as the precursor ion for CID (data not shown). In addition to the sulfated trisaccharide fragment, at m/z 622, from the non-reducing part, the spectrum of SM1a displayed the ion at m/z 419 which was consistent with the sulfated disaccharide $[(\text{HSO}_3\text{-O-Hex-O-Hex-O}) - 2\text{H}]^-$ from the reducing terminus. This ion at m/z 419, not present in its isomer SM1b, confirms that SM1a has a sulfated lactose unit next to ceramide, and excludes the alternative structure possessing a sulfate at the terminal hexose. In contrast, appearance of a series of sequential ions corresponding to the sulfated mono- to tri-saccharides in the spectrum of SM1b just as those in Fig. 5B reconfirmed that SM1b has a sulfate ester at the non-reducing terminus.

Low-energy CID.—SM1a, SM1b and SB1a were also analyzed by low-energy CID MS/MS. The $[\text{M} - \text{H}]^-$ or $[\text{M} - \text{SO}_3\text{H}]^-$ was selected as the precursor ion (Fig. 6). There were remarkable differences between high- and low-energy CID spectra. Only one major signal was abundantly produced for each mono-sulfated glycolipid, SM1a and SM1b; $[(\text{HSO}_3\text{-O-Hex-O-Hex-O-Cer}) - \text{H}]^-$ (m/z 1070) for SM1a (Fig. 6A) and $[(\text{HSO}_3\text{-O-Hex-O-HexNAc}) - \text{H}_2\text{O} - \text{H}]^-$ (m/z 444) for SM1b (Fig. 6B), indicating that SM1a has an internal sulfated disaccharide unit next to ceramide and SM1b has a terminal sulfated disaccharide. The spectra of SM1a and SM1b also displayed other minor product ions corresponding to the internal sulfated trisaccharides plus ceramide minus H_2O (m/z 1255 in Fig. 6A) and *N*-deacylated SM1b (lyso-form, m/z 1085 in Fig. 6B), respectively. In contrast, both of the ions, m/z 444 and m/z 1070, were observed for SB1a (Fig. 6C), confirming that SB1a has a sulfate ester on both an internal and the terminal saccharide residues.

Comparison of the high-energy CID-linked scan spectrum of SM1a presented here (Fig. 4) with that of GM1a [17,25,31], containing a sialic acid residue instead of a sulfate ester on the same gangliotetraose core, indicates the presence of similar product ions produced by the sequential cleavage of the glycosidic bonds and sugar ring cleavage. Additionally, these fragment ions always retained the sulfate ester or sialic acid residue. In contrast, the low-energy CID spectrum of SM1a (Fig. 6A) was completely different from that of GM1a [25]. In the low-energy CID of GM1a [25], several product ions with, or without, sialic acid residue were produced by the cleavage of the glycosidic bonds, while in the low-energy CID spectrum of SM1a (Fig. 6A), only one major product ion that retains sulfate ester was abundantly produced as noticed above. This remarkable difference indicates that, under high-energy CID for both GM1a and SM1a, the fragmentations would arise via charge-remote rather than charge-induced

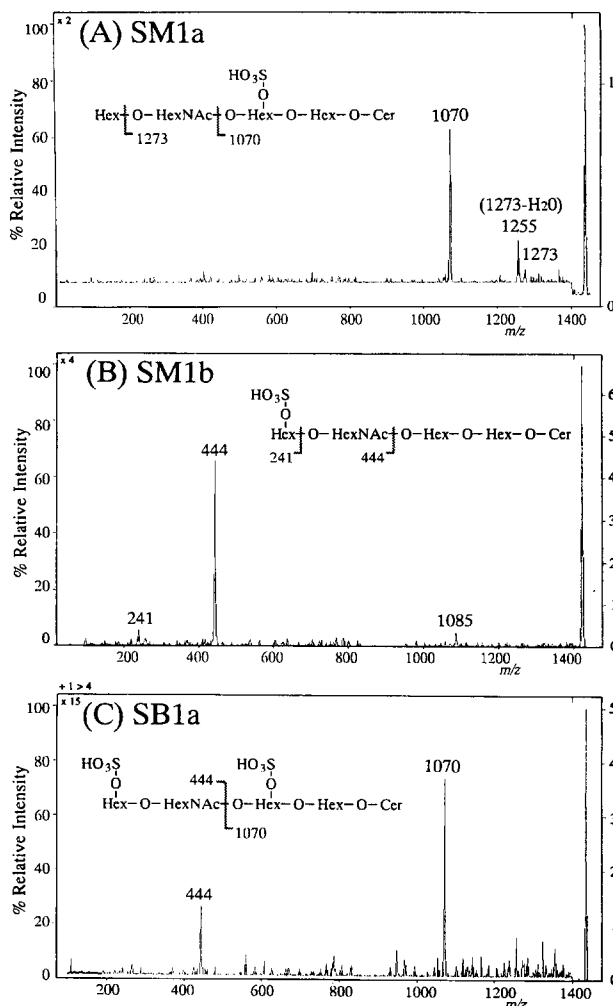


Fig. 6. Low-energy CID MS/MS product ion spectra of (A) SM1a, (B) SM1b, and (C) SB1a. The precursor ions are $[M-H]^-$ at m/z 1435 for SM1a (A) and 1451 for SM1b (B), and $[M-SO_3H]^-$ at m/z 1435 for SB1a (C).

cleavages. Under low-energy CID, on the contrary, the lack of CRF as well as the presence of fixed negative charge on sulfate would make the spectrum of SM1a extremely simple (Fig. 6A). Because the negative site of charge on sialic acid is not so rigid as that on sulfate, GM1a could fragment upon low-energy CID via charge-induced cleavages of the glycosidic bonds to give a rather complex spectrum [25].

Several reports on FAB mass spectrometry of glycolipids and saccharides described that permethylated samples gave more intense spectra and more easily interpretable fragment ions than underivatized samples [17,21,23,29,33]. LSIMS of these sulfated glycolipids after permethylation would be expected to give some additional useful fragments. In the present case, however, key information on the location of the sulfate

ester as well as molecular weight and saccharide sequence was provided by negative ion LSIMS and CID using native samples. For this strategy, the material requirement was less than 1 nmol. Although product ions obtained from low-energy CID by itself appeared to be insufficient for structural analysis of sulfated glycolipids, the fragmentation patterns are unique fingerprints of each structure. Thus, this sensitive strategy, combining LSIMS with high- and low-energy CID has proved useful in identifying the structures of sulfated glycolipids that differ in the position and the number of sulfate esters.

References

- [1] L. Svennerholm, *J. Neurochem.*, 10 (1963) 613–623.
- [2] A. Makita and N. Taniguchi, in H. Wiegandt (Ed.), *Glycolipids*, Elsevier, Amsterdam, 1985, pp 1–99.
- [3] K. Nagai, I. Ishizuka, and S. Oda, *J. Biochem. (Tokyo)*, 95 (1984) 1501–1511.
- [4] Y. Niimura and I. Ishizuka, *Biochim. Biophys. Acta*, 1052 (1990) 248–254.
- [5] Y. Niimura and I. Ishizuka, *Comp. Biochem. Physiol.*, 100B (1991) 535–541.
- [6] Yamakawa, N. Kiso, S. Handa, A. Makita, and S. Yokoyama, *J. Biochem. (Tokyo)*, 52 (1962) 226–227.
- [7] E. Martensson, *Biochim. Biophys. Acta*, 116 (1966) 521–531.
- [8] K. Tadano and I. Ishizuka, *J. Biol. Chem.*, 257 (1982) 1482–1490.
- [9] K. Tadano and I. Ishizuka, *J. Biol. Chem.*, 257 (1982) 9294–9299.
- [10] K. Tadano, I. Ishizuka, M. Matsuo, and S. Matsumoto, *J. Biol. Chem.*, 257 (1982) 13413–13420.
- [11] N. Iida, T. Toida, Y. Kushi, S. Handa, P. Fredman, L. Svennerholm, and I. Ishizuka, *J. Biol. Chem.*, 264 (1989) 5974–5980.
- [12] K. Tadano-Aritomi, T. Kasama, S. Handa, and I. Ishizuka, *Glycoconjugate J.*, 8 (1991) 168.
- [13] K. Tadano-Aritomi, T. Kasama, S. Handa, and I. Ishizuka, *Eur. J. Biochem.*, 209 (1992) 305–313.
- [14] K. Tadano-Aritomi, M. Okuda, I. Ishizuka, H. Kubo, and P. Ireland, *Carbohydr. Res.*, 265 (1994) 49–59.
- [15] Y. Kushi, S. Handa, and I. Ishizuka, *J. Biochem. (Tokyo)*, 97 (1985) 419–428.
- [16] V.N. Reinhold, in S.J. Gaskell (Ed.), *Mass Spectrometry in Biomedical Research*, Wiley, 1986, pp 181–213.
- [17] C.E. Costello and J.E. Vath, *Methods Enzymol.*, 193 (1990) 738–768.
- [18] B.L. Gillece-Castro and A.L. Burlingame, *Methods Enzymol.*, 193 (1990) 689–712.
- [19] J. Peter-Katalinic and H. Egge, *Methods Enzymol.*, 193 (1990) 713–733.
- [20] T. Matsubara and A. Hayashi, *Prog. Lipid Res.*, 30 (1991) 310–322.
- [21] A. Dell, A.J. Reason, K.-H. Khoo, M. Ranico, R.A. McDowell, and H.R. Morris, *Methods Enzymol.*, 230 (1994) 108–132.
- [22] I. Ishizuka and K. Tadano-Aritomi, *J. Biochem. (Tokyo)*, 96 (1984) 829–839.
- [23] H. Leffler, G.C. Hansson, and N. Stromberg, *J. Biol. Chem.*, 261 (1986) 1440–1444.
- [24] K. Tadano-Aritomi, T. Kasama, S. Handa, H. Kubo, P. Ireland, and I. Ishizuka, in T. Matsuo (Ed.), *Proceedings of the Kyoto '92 International Conference on Biological Mass Spectrometry*, San-ei Publishing Co., Kyoto, 1993, pp 326–327.
- [25] T. Kasama and S. Handa, *Biochemistry*, 30 (1991) 5621–5624.
- [26] T. Taketomi, A. Hara, Y. Kutsukake, and E. Sugiyama, *J. Biochem. (Tokyo)*, 107 (1990) 680–684.
- [27] B.W. Gibson and P. Cohen, *Methods Enzymol.*, 193 (1990) 480–501.
- [28] Y. Ohashi and Y. Nagai, *Carbohydr. Res.*, 221 (1991) 235–243.
- [29] K. Sugahara, Y. Takemura, M. Sugiura, Y. Kohno, K. Yoshida, K. Takeda, K.H. Khoo, H.R. Morris, and A. Dell, *Carbohydr. Res.*, 255 (1994) 165–182.
- [30] T. II, S. Okuda, T. Hirano, and M. Ohashi, *Glycoconjugate J.*, 11 (1994) 123–132.
- [31] B. Domon and C.E. Costello, *Biochemistry*, 27 (1988) 1534–1543.
- [32] J. Adams, *Mass Spectrom. Rev.*, 9 (1990) 141–186.
- [33] S.B. Levery, M.E.K. Salyan, E.D. Nudelman, and S. Hakomori, in A.L. Burlingame and J.A. McCloskey (Eds.), *Biological Mass Spectrometry*, Elsevier, Amsterdam, 1989, pp 495–508.